THE JOURNAL OF PHYSICAL CHEMISTRY C

Article

pubs.acs.org/JPCC

Selective Discrimination among Benzene, Toluene, and Xylene: Probing Metalloporphyrin-Functionalized Single-Walled Carbon Nanotube-Based Field Effect Transistors

Arti Dinkarrao Rushi,[†] Kunal Prasanta Datta,[†] Prasanta Sudarson Ghosh,[†] Ashok Mulchandani,[§] and Mahendra Dasharath Shirsat*[,†]

[†]Intelligent Materials Research Laboratory, Dr. Babasaheb Ambedkar Marathwada University, Aurangabad 431004, MS, India

[§]Department of Chemical and Environmental Engineering, University of California, Riverside, 900 University Avenue, Riverside, California 92521, United States

Supporting Information

ABSTRACT: Single-walled carbon nanotubes have been noncovalently functionalized with metalloporphyrins. Iron tetraphenyl porphyrin and cobalt tetraphenyl porphyrin were independently employed to functionalize aligned nanotubes network that formed the channel material for chemical field effect transistor-based sensors. The primary aim of the study was to achieve discrimination among structurally similar aromatic hydrocarbons, benzene, toluene, and xylene, and derive possible role of the central metal ions present in the metalloporphyrins in defining sensor selectivity. Current−voltage and field effect transistor measurements have confirmed formation of the efficient charge transfer complex during functionalization. The sensors were validated in respect to the analyte atmosphere within a concentration window of 500 ppb to 10 ppm. A clear affinity of the sensors toward toluene was recorded; however, the iron tetraphenyl porphyrin functionalized sensors exhibited a clear response (change in normalized resistance = 0.728) at lowest concentration validated, approximately 30% sensitivity (500 ppb to 10 ppm concentration) and excellent linearity (R^2 =0.94) with figures that are significantly better than cobalt tetraphenyl porphyrin-based devices. Observed behavior of the sensors have been rationalized in terms of vacant d orbitals of the central metal ions of metalloporphyrins and the side substituents present in the structure of the hydrocarbons validated.

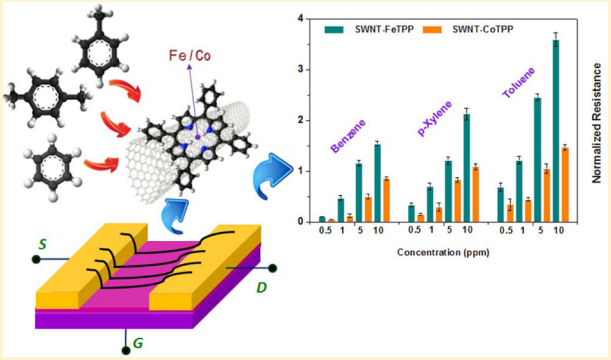

INTRODUCTION

Selective quantification of analytes at low concentration has been one of the challenges in designing efficient gas sensor platforms. Systematic investigation[1] is therefore required for reliable quantitative determination of analytes with similar structure. From this standpoint, aromatic organic compounds (AOC), especially benzene (C_6H_6) and its alkyl derivatives, toluene (C_7H_8) and xylenes [or the three isomers of dimethylbenzene C_6H_4 $(CH_3)_2$)], have gained significant research interest[2,3] due to their obvious presence in environment[4,5] and hazardous effects on human health.[6]

A prominent representative group of aromatic hydrocarbons, benzene, toluene, and xylene (BTX), are considered to be among highly hazardous volatile pollutants. These are mainly produced from automobile exhausts[7,8] and incomplete combustion of fossil fuels.[9] BTX constitute the mainframe of petrochemical materials and are widely found in gasoline, thinner, and solvents for several chemical reactions.[10,11] Numerous consumer and agricultural products, especially pesticides contain component(s) of BTX.[12] Natural sources (e.g., landfill leachate) is another potential source of various toxic organic compounds in which BTX are among prime components.[13] The toxic,[14] carcinogenic,[15] and neurological effects of the BTX[16] are well-established, and the adverse health effects are too slow for early determination. Hence, reliable sensing of BTX seeks serious attention.

Sensitive detection of BTX components reported to date have mostly been carried out by quartz crystal microbalance (QCM)-based sensors.[17−20] Other approaches that have shown encouraging results include sensors based on optical planar Bragg grating,[9] conducting polymer,[21,22] and spectroscopic measurements.[23−25] However, most of these approaches have rarely taken into account the issue of sensor affinity toward components of BTX. Moreover, the noticeable discrepancy in selectivity of the reported sensors is a strong motivation for study in this direction. For example, while QCM modified with β- cyclodextrin polymer thin film[19] and poly(methyl methacrylate) (PMMA) with a plasticizer[20] exhibited better sensing

Received: May 12, 2014
Revised: September 18, 2014
Published: September 22, 2014

   dx.doi.org/10.1021/jp504657c | J. Phys. Chem. C 2014, 118, 24034−24041

for *p*-xylene, a quartz crystal nanobalance (QCN) modified with polystyrene[26] exhibited better sensitivity toward toluene. Therefore, a need of efforts toward proper understanding of such differences in observations is highly necessary for real-time BTX sensors with high sensitivity and selectivity.

Advancing research efforts toward development of a volatile organic compounds (VOCs) sensor, our group has demonstrated simple chemiresistive backbones constituted of noncovalently functionalized single-walled carbon nanotubes (SWNTs) with metalloporphyrins (MPs) for sensitive detection of VOCs.[27,28] Basically, the presence of an aromatic π-system in BTX suggests that functional moieties that possess a π-system (for example, porphyrins) are able to induce $\pi-\pi$ interaction with the benzene ring of BTX that facilitates their detection.[29] As a matter of fact, porphyrins/MPs have been explored in QCM modality for detection of aromatic hydrocarbons.[30,31] Yet, the complexity of the QCMs always asks for simpler detection technique that has directed the exploration of modulation in electrical characteristics of this class of materials under exposure to toxic VOCs. Any encouraging outcome, however, was highly impeded by the poor electrical conductivity of porphyrins/MPs.[32] In this context, noncovalent functionalization of SWNTs with MPs has been found to be highly effective. The potential of SWNTs as a sensing material is widely reported,[33] especially, in terms of their high aspect ratio that makes them act as molecular wires. At the same time, the SWNTs are reported to be weakly sensitive to VOCs.[34] By noncovalent functionalization with MPs, on one hand, the surface electronic properties of the SWNTs are retained and on the other hand, specific affinity of the MPs (by dint of the variation in side substituents and central metal atom) toward different VOCs could be capitalized by virtue of the extensive $\pi-\pi$ delocalization[27] at MP/SWNTs interfacial sites.

Our group has already reported that central metal ion in MPs plays a decisive role in enhancing sensor behavior[28] where we had observed that iron tetraphenyl porphyrin (FeTPP)-functionalized SWNTs sensor exhibited better sensing performance toward benzene in comparison to tetraphenyl porphyrin (TPP)-functionalized SWNTs sensor. Toward further confirmation of our findings and to probe selectivity characteristics, the present course of investigation has been directed to (i) define possible affinity of MP-functionalized SWNTs toward analytes with similarity in chemical structure (BTX in this case) and (ii) evaluate the role of the transition metal present at the center of MPs ring in deciding sensor selectivity.

In the present investigation, chemical field effect transistors (ChemFET) have been fabricated with aligned SWNTs network functionalized independently with iron tetraphenyl porphyrin (FeTPP) and cobalt tetraphenyl porphyrin (CoTPP) as channel materials. Choice of the central metal ions (Fe and Co) in this case was judicious where the partially vacant d-orbitals of the ions were a point of interest. The sensors were validated in respective analyte atmosphere within a concentration window of 500 ppb to 10 ppm. A low concentration range was purposefully chosen so as to study the sensing capabilities for low concentration occurrence of the analytes. A clear affinity of the sensors toward toluene was recorded for both the porphyrins; however, the FeTPP-functionalized sensors exhibited sensing behavior that was significantly better than CoTPP-based devices. Our observations indicate that apart from the central metal ion of MPs, the structure of aromatic hydrocarbons frames an important point of interest while considering selectivity issue of the fabricated sensors. The inherent general significance of the observations is the fact that sensors based on electron transfer mechanism can be inculcated with selectivity even for electron-donating analytes.

EXPERIMENTAL DETAILS

Sensor Substrate. Highly p-doped Si (525 nm) formed the base layer of the substrate on which 100 nm SiO_2 layer was grown by low-pressure chemical vapor deposition. Chromium (Cr; 20 nm) and gold (Au; 180 nm) were then subsequently deposited by e-beam and thermal evaporation, respectively. Micro patterns were finally generated by standard lift-off and photolithography technique.[35] Electrodes were designed to be 200 μm in width with a 3 μm gap between adjacent Au fingertips. Substrates were ultrasonically cleaned in acetone prior to use.

Materials. SWNTs with COOH moieties (COOH-SWNTs) were procured from Nanoshel LLC. Both FeTPP and CoTPP (99% purity) were purchased from Sigma-Aldrich (Switzerland). Solutions of SWNTs, FeTPP, and CoTPP were prepared in *N*,*N*-dimethylformamide (*N*,*N*-DMF, GC grade) obtained from Rankem (India) Ltd.

Sensor Fabrication. Primary SWNTs backbone were obtained by bridging 3 μm apart microelectrode structures with dielectrophoretically aligned SWNTs.[27,28] A homogeneous dispersion of COOH-SWNTs in *N*,*N*-DMF was first obtained by ultrasonication at medium power level (VWR 100C ultrasonic bath; 0.41 mg SWNTs in 20 mL *N*,*N*-DMF) followed by centrifugation at 15000 rpm for 90 min. Decanted suspension was stocked for further use under ambient conditions. Prior to use, a requisite amount of the stock suspension was sonicated for 30 min, and a 0.2 μL drop of the same was placed in between Au microelectrodes. Dielectrophoretic alignment was carried out under 1.5 V_{p-p} (sinusoidal) AC signal at 4 MHz frequency. Resistance of the devices were optimized by controlling the duration of the applied signal. After preliminary drying of the devices in N_2 atmosphere, annealing was carried out in a reducing atmosphere (300 °C; 5% H_2 + 95%N_2) to obtain better contact between SWNTs and Au microelectrodes.[28]

For functionalization of pristine-aligned SWNTs, separate 0.1 mM solutions of FeTPP and CoTPP were prepared in *N*,*N*-DMF by continuous stirring for 30 min at room temperature. Functionalization was carried out by the simple drop-casting route. A 0.4 μL of the desired porphyrin solution was placed on the pristine SWNT sensor device for 30 min followed by wash under nanopure water and annealing at 90 °C in N_2 atmosphere for 60 min. All measurements were carried out under standard laboratory conditions (25± 1 °C, 35−40% R_H) unless stated otherwise.

CHARACTERIZATIONS AND INSTRUMENTATION

Field Emission Scanning Electron Microscopy (FESEM) images were recorded with Hitachi S-4800. Elemental component analysis was done by EDAX spectrum obtained from the same machine. UV−vis spectroscopic studies were carried out with Shimadzu UV−vis 2450 spectrophotometer.

To study the electrical properties of the fabricated sensors, CHI 660C electrochemical workstation (CH Instruments) was employed. *I*−*V* characteristics of pristine as well as functionalized devices were carried out by a linear sweep voltammetry technique, where voltage was swept from −1 to +1 V under a

dx.doi.org/10.1021/jp504657c | J. Phys. Chem. C 2014, 118, 24034−24041

0.01 V s^{-1} scan rate. FET transfer characteristics of pristine and metalloporphyrin-functionalized SWNT devices were studied in back gate configuration with Keithley 2400 (Keithley) source measure unit in conjunction with a programmable power supply (PPD3003-S; Aplab, India). While studying transfer characteristics, gate voltage was swept from −20 to +20 V at a scan rate of 0.1 V s^{-1}, while drain to source voltage was kept constant at −1 V.

Sensing performances of the fabricated devices were studied in an indigenously designed dynamic gas sensing setup. The sensor devices were wire-bonded (7476D, Wedge Bond West Bonder) to a custom chip carrier, and the assembly was kept in a flow cell having a volume of approximately 8 cm^3. Before the actual sensing behavior was studied, the sensors were exposed to dry air until a stable baseline resistance could be achieved. ChemFET transfer measurements were carried out for elucidation of the sensing mechanism under 1 ppm concentration of the respective analyte. Experimental set up for the same was identical to that employed for studying transfer characteristics already described. For real-time analysis, sensors were subjected to various concentrations of BTX separately. Requisite concentrations of analytes were prepared by diluting them in dry air (carrier), while the cumulative flow rate was kept to be 200 sccm. Under a constant drain to source voltage (V_{DS}) equal to −1 V, the changes in channel current (I_{DS}), as a function of various concentrations of analyte, was recorded by a computer controlled source-measure unit (KEITHLEY 2400) while the gate to source voltage (V_{GS}) was maintained at −14 V for the SWNT-FeTPP sensor and −15 V for the SWNT-CoTPP sensor. At least 5 devices were validated in each case for studying device-to-device variation.

RESULTS AND DISCUSSION

Field Emission Scanning Electron Microscopy (FESEM) and Energy Dispersive X-ray Analysis (EDAX). The FESEM image, as given in Figure 1a, confirms the alignment

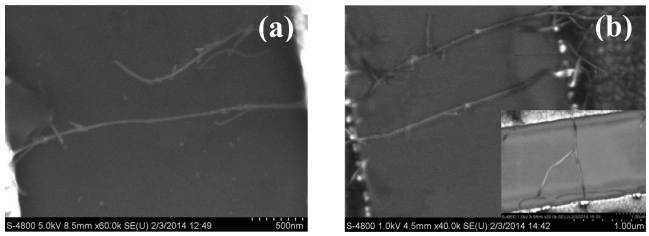

Figure 1. FESEM image of (a) aligned SWNTs, (b) aligned SWNTs functionalized by FeTPP and annealed at 90 °C, and (inset) aligned SWNTs functionalized by FeTPP before annealing.

of the SWNTs. After functionalization with FeTPP, an increment of ∼22 nm in diameter could be observed (Figure 1b inset). After annealing, ∼10 nm decrease in diameter was observed as compared to devices without annealing, as estimated from Figure 1b. By and large, the coating layer was found to be uniform. As annealing was found to be an effective tool to optimize the coating of the MPs over the SWNTs, only annealed devices were used for further experiment.

EDAX spectra of the FeTPP- and CoTPP-functionalized SWNTs based devices (Figure 2, panels a and b) clearly confirmed the presence of Fe and Co in FeTPP-SWNTs and CoTPP -SWNTs structures, respectively.

UV−vis Spectroscopy. Figure 3 shows the UV−vis spectra of pristine SWNTs, FeTPP, and SWNT-FeTPP suspensions. For SWNTs, the characteristic spectra exhibited only one absorption peak at 276 nm, indicating a $\pi-\pi^*$ transition of electrons. In the case of FeTPP, broad Soret peak observed in the range of 270−400 nm arises due to strong transition to the second excited state (S_0 to S_2). Q-band was observed at 566 nm due to weak transition to the first excited state (S_0 to S_1). Both these excitations resulted from a $\pi-\pi^*$ transition of electrons.[36] For SWNT-FeTPP suspension, the absorption peak at 276 nm and specifically the decrease in absorbance in the range of 270−350 nm possibly confirm the formation of complex. A blue shift observed in the Q-band of the SWNT-FeTPP from 566 (in FeTPP) to 530 nm is another probable indication of the complex formation.

Current−Voltage (*I*−*V*) and Field Effect Transistor (FET) Transfer Characteristics. Current−voltage ($I-V$) characteristics, apart from depicting the electrical conduction behavior of the fabricated devices, confirmed the formation of the SWNT-FeTPP/CoTPP charge transfer complex. $I-V$ characteristics of the pristine and functionalized SWNTs devices are given in Figure 4. Highest device current was observed for pristine SWNTs-based devices. Such devices have also demonstrated an "S" nature that is a possible indication of the formation of Schottky barriers at the SWNTs/Au junction, signifying the presence of semiconducting SWNTs.[35,37,38] After functionalization, the device current was found to decrease for both FeTPP- and CoTPP-functionalized devices. This decrease in device current could be well-attributed to the possible donation of electrons from respective MPs to the p-type SWNTs backbone.[39] The degree of decrease in device current was observed to be more profuse with CoTPP-functionalized devices. This observation might be rationalized in terms of the higher number of d-orbital electrons in Co in comparison to Fe, resulting in enhanced electron donation from MPs to SWNTs backbone for CoTPP-based devices.

Figure 5 shows the FET transfer characteristics of the pristine SWNTs, SWNTs-FeTPP, and SWNTs-CoTPP devices.

As evident from the transfer characteristics, there has been (i) clear negative shifts in device threshold voltage (V_{TH}) and (ii) lowering of device current (I_{DS}) with the functionalized devices in comparison to the pristine SWNTs-based device. The CoTPP-functionalized devices were characterized with lowest I_{DS} and maximum negative shift in V_{TH}. The V_{TH} for a CoTPP-based device was found to be −07 V, figuring a shift of −04 V with respect to pristine SWNTs-based devices. In contrast, the FeTPP-based device exhibited a shift of −03 V. Thus, in line to our observations with $I-V$ characteristics, the transfer characteristics also confirm donation of electrons from respective MPs to sensor backbone, resulting in recombination with holes in SWNTs. The effective decrease in hole concentration with respect to a pristine SWNTs-based device were estimated to be $\sim 43 \times 10^{12}$ and $\sim 57 \times 10^{12}$ cm^{-1} (see Supporting Information) for functionalization with FeTPP and CoTPP, respectively. The difference in hole concentration certainly justifies the higher negative shift in V_{TH} observed for CoTPP-functionalized device. Since a lower hole concentration facilitates depletion of channel from majority charge carriers (holes in this case) at lesser V_{TH}, the maximum negative shift observed for CoTPP functionalization stands justified. Certainly, a lower hole concentration also implies that the device current for CoTPP-functionalized device is minimum. The mobility values of pristine SWNTs and functionalized

dx.doi.org/10.1021/jp504657c | J. Phys. Chem. C 2014, 118, 24034−24041

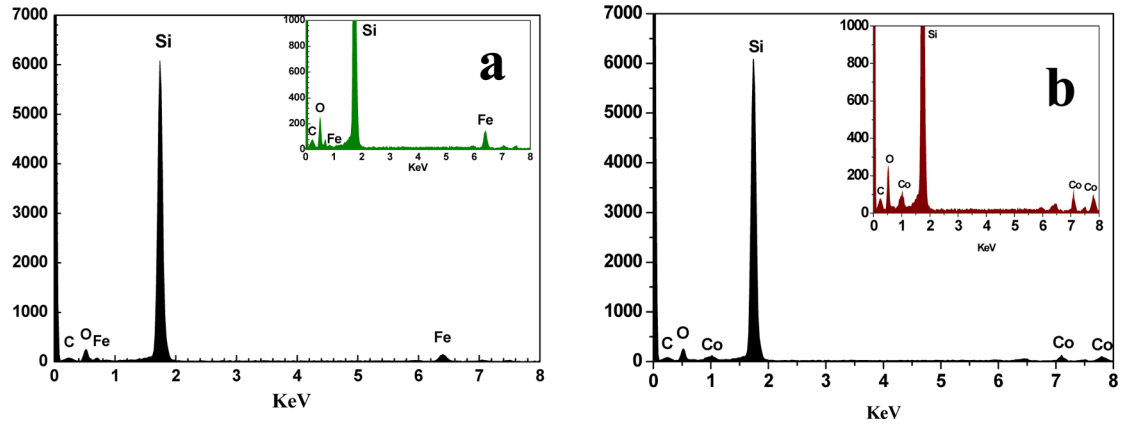

Figure 2. (a) EDAX spectrum of FeTPP-functionalized SWNTs, (b) EDAX spectrum of CoTPP functionalized SWNTs, and (inset) magnified version of the same.

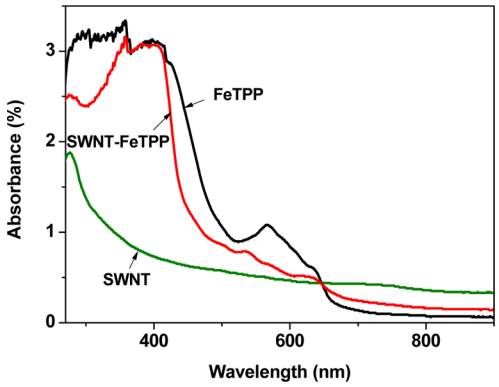

Figure 3. UV −Vis spectra of SWNTs, FeTPP, and SWNT-FeTPP.

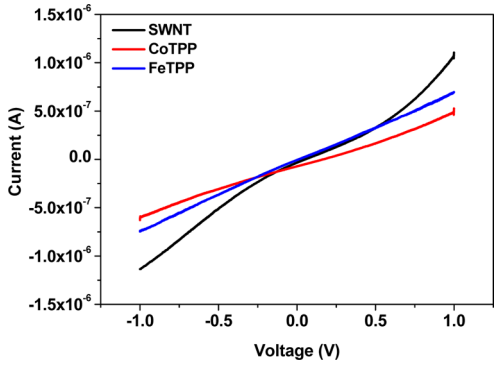

Figure 4. *I*−*V* Characteristics of SWNT, SWNT-FeTPP, and SWNT-CoTPP sensor(s).

devices were also estimated (see the Supporting Information). The mobility for SWNT-FeTPP device was found to be ∼5.96 × 10^{-2} cm^2 $V^{-1}s^{-1}$, whereas for the SWNT-CoTPP device, mobility was recorded to be ∼5.5 × 10^{-2} cm^2 V^{-1} s^{-1} in comparison to 6.5 × 10^{-2} cm^2 V^{-1} s^{-1} for a pristine SWNT device.[40] The results certainly confirm the formation of charge transfer complex after functionalization.

ChemFET Sensing. Transfer characteristics of the FeTPP- and CoTPP-functionalized sensors, upon exposure to 1 ppm concentration of each of the BTX component are shown in Figure 6. After exposure to analytes, both the sensors have exhibited clear negative shifts in the respective threshold voltages (V_{TH}) with respect to dry air (reference). Most

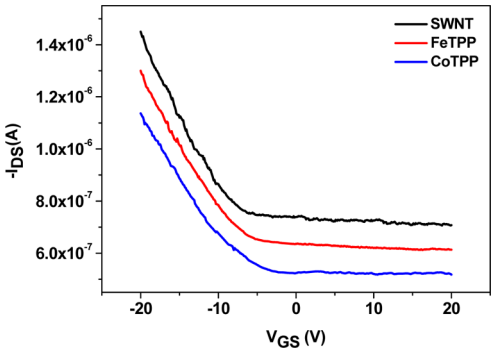

Figure 5. Field Effect Transistor (FET) Characteristics of the SWNT and FeTPP- and CoTPP-functionalized sensors.

possibly, these "shifts" could be due to electron donation from analytes to the sensor backbone.[40,41] Also, no significant change could be noted in the slope of the transfer curves after exposure to any of the analytes, confirming that there had been no major change in the contact properties of Au and SWNT-FeTPP- or CoTPP-functionalized sensors under the validated analyte atmosphere(s), and therefore, no Schottky barrier modulation[42] had taken place. Thus, the observed threshold voltage shifts are purely due to electrostatic gating[42] resulted by donation of electrons from analytes to the ChemFET channel. A closer look to the shifts in V_{TH} of the sensors show that for FeTPP-functionalized sensors, the changes were more significant than the CoTPP-functionalized sensors to an appreciable measure. Again, for both sensors, the shifts in V_{TH} were at a maximum for toluene followed by *p*-xylene and benzene. Our observations are indicative of certain facts that (i) the donated electrons (from analyte) recombine with holes of the p-type channel and thus the channel could be depleted of the majority charge carriers at lower threshold voltages with respect to dry air, under analyte exposure, and (ii) there is a significant difference in electron-donating capacity of the analytes in the order of toluene > *p*-xylene > benzene.

To have a quantitative substantiation of our inferences, estimation of the decrease in hole concentrations of the FeTPP- and CoTPP-functionalized sensors were carried out (see Supporting Information). Figure 7 reflects the decrease in hole-concentration figures (estimated over at least five devices) against each analyte for the sensors. Most interestingly, in inclination to the trends observed in transfer curves, it could be noted that (i) both the devices have suffered maximum

dx.doi.org/10.1021/jp504657c | J. Phys. Chem. C 2014, 118, 24034−24041

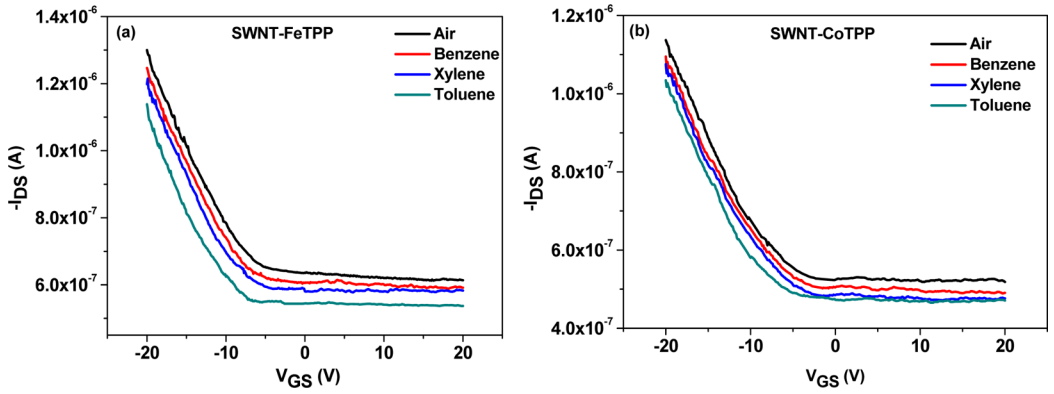

Figure 6. ChemFET sensing characteristics of (a) SWNT-FeTPP and (b) SWNT-CoTPP sensor toward benzene, *p*-xylene, and toluene at 1 ppm concentration of analyte.

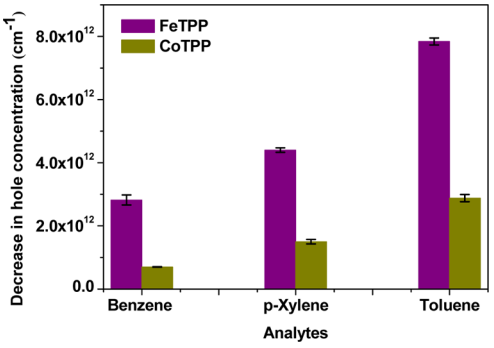

Figure 7. Decrease in carrier concentration (with respect to dry air) of SWNT-FeTPP and SWNT-CoTPP sensors after exposure to 1 ppm concentration of analyte (observations reflect results from at least five devices in each case).

decrease in hole concentration for toluene, followed by *p*-xylene and benzene and (ii) the effects are more profuse for FeTPP-functionalized sensors.

Real-Time Sensing Characteristics. Figure 8a shows the real-time response of the FeTPP-SWNT sensor in terms of changes in normalized resistances ($\Delta R/R_0$, where ΔR = change in resistance of the sensor under analyte exposure with respect to baseline resistance; R_0 = baseline resistance of the sensor) toward various concentrations of the analytes at V_{DS} = −1 V and V_{GS} = −14 V. All three analytes could be detected significantly below the PEL concentrations (benzene, 1 ppm; toluene, 200 ppm; and xylene, 100 ppm) with response−recovery cycle duration of less than 100 s within the entire window of validation, a significant point to make the sensors potential for real time, on-field operations. The devices could be characterized with rapid increase in sensor resistance on exposure to analytes and clear recovery behavior during refresh cycle under dry air atmosphere. The real time responses of the SWNT-CoTPP (Figure 8b) sensor were recorded at V_{DS} = −1 and V_{GS} = −15 V. The generic behavior of the CoTPP-based sensor was equivalent to the FeTPP-based sensor; however, the changes in normalized resistance was found to be distinctly lower for the CoTPP-based device. Also, at the lowest validated concentration (500 ppb), the response of device was not reliable. Calibration plots of the FeTPP device responses to the 500 ppb to 10 ppm window of all three analytes are shown in Figure 9a. Best sensing characteristics could be observed for toluene with a sensitivity of ∼30% with excellent linearity (R^2 value = 0.94) within the investigated window of concentration for the FeTPP-functionalized sensor.

Figure 9b shows calibration plots for CoTPP-functionalized devices. Sensitivity of the device for all analytes was significantly lower than that of FeTPP-functionalized devices, although the trend was similar. Most significantly, for the FeTPP-based device, the sensors showed a higher sensitivity to toluene in comparison to other analytes. Such affinity characteristic was absent for the CoTPP-based sensor.

The overall comparative performance of fabricated sensors is given in Figure 10. Device-to-device variation was found to be very trivial as reflected from Figures 9 and 10.

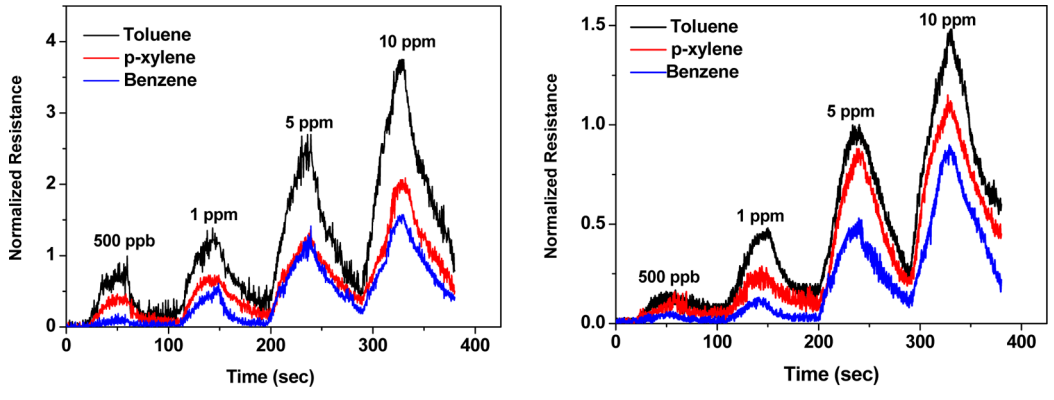

Figure 8. Real-time response characteristics of the (a) SWNTs-FeTPP and (b) SWNTs-CoTPP sensors.

dx.doi.org/10.1021/jp504657c | J. Phys. Chem. C 2014, 118, 24034−24041

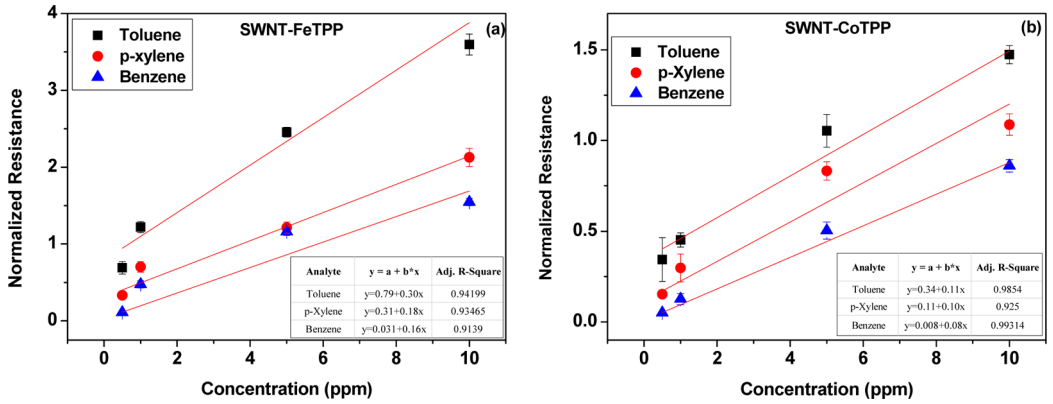

Figure 9. Calibration plot of (a) SWNT-FeTPP and (b) SWNT-CoTPP device (observations reflect results from at least five devices in each case).

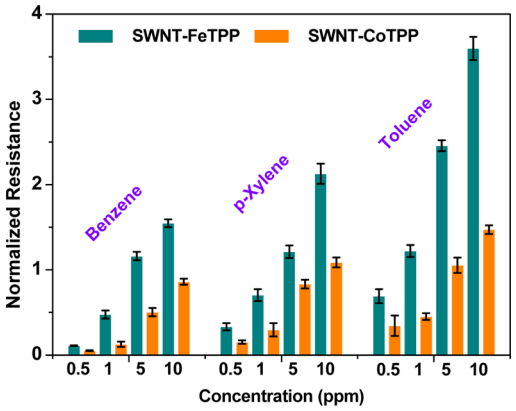

Figure 10. Comparative performance of the fabricated sensors.

In order to rationalize our findings, the d orbital electronic configurations of Fe ([Ar] $3d^6$ $4s^2$) and Co ([Ar] $3d^7$ $4s^2$) were considered. From that standpoint, the better sensing performance of the FeTPP-based device could be attributed to the higher vacancy in the d-orbital of Fe that renders better acceptability of electrons (than Co) from electron donating species. This possible inference further justifies our earlier observation where we have reported that the partially vacant d orbital of the central metal of MPs play important role in deciding sensor performance.[28] Elucidation of the similar trend in sensing performance with toluene, *p*-xylene, and benzene for both the sensors lead toward consideration of the structural aspects of analytes. Since the prime constituent of the analytes is the benzene ring, the role of the side substituents present in the ring for each of the analytes were evaluated. In the case of toluene, the presence of the alkyl ($-CH_3$) group at the ortho position effects in increase of electron density at the para and meta positions[43] of the ring, offering a higher electron-donating capacity in toluene than benzene that contains no side substitution. This may be the plausible reason that the fabricated sensors have responded better for toluene with respect to benzene. An intermediate performance of the sensors for *p*-xylene finds is a probable explanation in terms of the two alkyl substituents at ortho and para positions of the ring that decreases the effective electron density present on the ring in comparison to toluene. Therefore, it may be inferred that the central metal ion present in a metalloporphyrin ring and the structural characteristics of an aromatic hydrocarbon are the major issues that need sensitive consideration to achieve sensor selectivity.

CONCLUSION

Metalloporphyrins (FeTPP and CoTPP)-functionalized aligned SWNTs-based room temperature sensors for benzene, toluene, and *p*-xylene have been successfully fabricated with a facile drop casting method. Annealing of the functionalized sensors was found to be possibly improving the π-delocalization at the MP-SWNT interfacial sites, rendering excellent sensing characteristics. The structural and spectroscopic studies confirmed the functionalization, whereas electrical and FET measurements elucidated the formation of charge transfer complex with the electron donating nature of MPs. Room temperature ChemFET sensing revealed that toluene was better detected by both the sensors; however, with FeTPP functionalized devices, significantly better sensing performance could be achieved. Differences in electron-donating capabilities of the analytes, the prime responsible factor for inculcating selective nature to the sensors, have been rationalized in terms of the directive behavior of the side substituent(s) present in the primary benzene ring of the analytes. Also, the electronic configuration of the d-orbital of central metal ion has been found to be another crucial factor in deciding sensor performance where MPs with central transition metal ion is involved. The salient point of the findings lies with the fact that even for electron-donating analytes and sensors based on electron transfer mechanism, selective sensor performance is possible. Although the present study is based on aromatic hydrocarbons with structural similarity, directions may open up toward selective sensors for an inorganic class of analytes in the line of their structural formation. During the present course of investigations, the best sensor could be achieved for toluene as an analyte with a FeTPP-functionalized SWNTs backbone. The typical value of sensitivity of such sensors is ~30% with a linearity factor (R^2) of 0.94 in the concentration window of 500 ppb to 10 ppm. The fabricated sensors have shown significantly good response and recovery behavior in the validated range of concentration of the analytes. In conjunction with adequate electronic intelligence, such sensors can render potent platforms for real-time complex operations. The absolute standalone selectivity, however, warrants more stringent validation of the sensors in complex reference of analytes.

ASSOCIATED CONTENT

Supporting Information

Details of computation of hole concentration and charge carrier mobility. This material is available free of charge via the Internet at http://pubs.acs.org.

dx.doi.org/10.1021/jp504657c | J. Phys. Chem. C 2014, 118, 24034−24041

AUTHOR INFORMATION

Corresponding Author

*E-mail: mdshirsat@gmail.com and mds_bamu@yahoo.co.in. Tel: +91 240 2403386. Fax: +91 240 2403113.

Notes

The authors declare no competing financial interest.

ACKNOWLEDGMENTS

Authors express their sincere thanks to the Nanomission, Department of Science and Technology (India), for financial assistance under Project SR/NM/NS-94/2009 dated 09.09.2010.

REFERENCES

(1) Espinoza, J.; Sazhnikov, V.; Sabik, S.; Ionov, D.; Smits, E.; Kalathimekkad, S.; Steenberge, G.; Altimov, M.; Posniak, M.; Schoo, H. Flexible Optical Chemical Sensor Platform for BTX, 14th International Meeting on Chemical Sensors, Nuremberg, Germany, May 20−23, 2012; AMA Service GmbH: Wunstorf, Germany, 2012, 10.5162/IMCS2012/7.5.4

(2) Su, F.; Lu, C.; Hu, S. Adsorption of Benzene, Toluene, Ethylbenzene and p-Xylene by NaOCl-Oxidized Carbon Nanotubes. *Colloid Surf., A* **2010**, *353*, 83−91.

(3) David, P.; Pauls, R. Comparison of Sampling and Analysis Methods for Measurement of Airborne Aromatic Hydrocarbons in Operating Petrochemical Plants. *J. Chromatogr. Sci.* **1998**, *36*, 44−48.

(4) Mottaleb, M.; Abedin, M.; Islam, M. Determination of Volatile Organic Compounds in River Water by Solid Phase Extraction and Gas Chromatography. *J. Environ. Sci.* **2004**, *16*, 497−501.

(5) Koch, R.; Knispel, R.; Elend, M.; Siese, M.; Zetzsch, C. Consecutive Reactions of Aromatic−OH Adducts with NO, NO_2 and O_2: Benzene, Toluene, m- and p-Xylene, Hexamethylbenzene, Phenol, m-Cresol and Aniline. *Atmospheric Chemistry and Physics Discussions* **2006**, *6*, 7623−7656.

(6) Fally, S.; Carleer, M.; Vandaele, A. UV Fourier Transform Absorption Cross Sections of Benzene, Toluene, meta-, ortho- and para-Xylene. *J. Quant. Spectrosc. Radiat. Transfer* **2009**, *110*, 766−782.

(7) Singh, A. K.; Neetu, T.; Jain, C. L. Monitoring, Assessment and Status of Benzene, Toluene and Xylene Pollution in the Urban Atmosphere of Delhi, India. *Res. J. Chem. Sci.* **2012**, *2*, 45−49.

(8) Bahrami, A.; Mahjub, H.; Sadeghian, M.; Golbabaei, F. Determination of Benzene, Toluene and Xylene (BTX) Concentrations in Air Using HPLC Developed Method Compared to Gas Chromatography. *International Journal of Occupational Hygiene* **2011**, *3*, 12−17.

(9) Girschikofsky, M.; Rosenberger, M.; Belle, S.; Brutschy, M.; Waldvogel, S. R.; Hellmann, R. Optical Planar Bragg Grating Sensor for Real-time Detection of Benzene, Toluene and Xylene in Solvent Vapour. *Sens. Actuators, B* **2012**, *171*, 338−342.

(10) Ferrando, M. D.; Andreu-Moliner, E. Acute Toxicity of Toluene, Hexane, Xylene, and Benzene to the Rotifers Brachionus Calyciflorus and Brachionus Plicatilis. *Bull. Environ. Contam. Toxicol.* **1992**, *49*, 266−271.

(11) Camou, S.; Tamechika, E.; Horiuchi, T. Portable Sensor for Determining Benzene Concentration from Airborne/ Liquid Samples with High Accuracy. *NTT Tech. Rev.* **2012**, *10*, 1−7.

(12) Kandyala, R.; Raghavendra, S.; Rajasekharan, S. Xylene: An Overview of Its Health Hazards and Preventive Measures. *Int. J. Oral Maxillofac. Pathol.* **2010**, *14*, 1−5.

(13) Silva, L.; Panteleitshouck, A.; Freitas, A.; Rocha-Santos, T.; Duarte, A. C. Microscale Optical Fibre Sensor for BTEX Monitoring in Landfill Leachate. *Anal. Methods* **2009**, *1*, 100−107.

(14) Pyta, H. BTX Air Pollution in Zabrze, Poland. *Pol. J. Environ. Stud.* **2006**, *15*, 785−791.

(15) McMichael, A. J. Carcinogenicity of Benzene, Toluene and Xylene: Epidemiological and Experimental Evidence. *IARC Sci. Publ.* **1988**, *85*, 3−18.

(16) Mandiracioglu, A.; Akgur, S.; Kocabiyik, N.; Sener, U. Evaluation of Neuropsychological Symptoms and Exposure to Benzene, Toluene and Xylene among Two Different Furniture Worker Groups in Izmir. *Toxicol. Ind. Health* **2011**, *9*, 802−809.

(17) Pejcic, B.; Myers, M.; Ranwala, N.; Boyd, L.; Baker, M.; Ross, A. Modifying the Response of a Polymer-Based Quartz Crystal Microbalance Hydrocarbon Sensor with Functionalized Carbon Nanotubes. *Talanta* **2011**, *15*, 1648−1657.

(18) Macagnano, A.; Sgreccia, E.; Paolesse, R.; Casare, F.; Amico, A.; Natale, C. Sorption and Condensation Phenomena of Volatile Compounds on Solid-State Metalloporphyrin Films. *Sens. Actuators, B* **2007**, *124*, 260−268.

(19) Ju, J. F.; Syu, M. J.; Teng, H. S.; Chou, S. K.; Chang, Y. S. Preparation and Identification of β-Cyclodextrin Polymer Thin Film for Quartz Crystal Microbalance Sensing of Benzene, Toluene, and *p*-Xylene. *Sens. Actuators, B* **2008**, *132*, 319−326.

(20) Pejcic, B.; Crooke, E.; Boyd, L.; Doherty, C.; Hill, A.; Myers, M.; White, C. Using Plasticizers to Control the Hydrocarbon Selectivity of a Poly(methyl met hacrylate)-Coated Quartz Crystal Microbalance Sensor. *Anal. Chem.* **2012**, *84*, 8564−8570.

(21) Barisci, J. N.; Wallace, G.; Andrews, M.; Partridge, A.; Harris, P. Conducting Polymer Sensor for Monitoring Aromatic Hydrocarbons Using an Electronic Nose. *Sens. Actuators, B* **2002**, *84*, 252−257.

(22) Li, W.; Hoa, N.; Cho, Y.; Kim, D.; Kim, J. Real Time Monitoring of Benzene, Toluene and p-Xylene in a Photoreaction Chamber With a Tunable Mid-Infrared Laser and Ultraviolet Differential Optical Absorption Spectrioscopy. *Sens. Actuators, B* **2009**, *143*, 132−138.

(23) Parsons, M.; Sydoryk, I.; Lim, A.; Mclntyre, T.; Tulip, J.; Jager, W.; McDonald, K. *Appl. Opt.* **2011**, *50*, 90−99.

(24) Hirschmann, C. B.; Sinisalo, S.; Uotila, J.; Ojala, S.; Keiski, R. L. Trace Gas Detection of Benzene, Toluene, *p*-, *m*- and *o*-Xylene with a Compact Measurement System using Cantilever Enhanced Photoacoustic Spectroscopy and Optical Parametric Oscillator. *Vib. Spectrosc.* **2013**, *68*, 170−176.

(25) Silva, A.; Pimentel, M.; Raimundo, I., Jr.; Almeida, Y. A PVC Sensing Phase for Determination of BTEX in Water Employing Mid-infrared Spectroscopy. *Vib. Spectrosc.* **2008**, *46*, 39−44.

(26) Mirmohseni, A.; Rostamizadeh, K. Quartz Crystal Nanobalance in Conjunction with Principal Component Analysis for Identification of Volatile Organic Compounds. *Sensors* **2006**, *6*, 324−334.

(27) Shirsat, M.; Sarkar, T.; Kakoullis, J.; Myung, N.; Konnanath, B.; Spanias, A.; Mulchandani, A. Porphyrin-Functionalized Single-Walled Carbon Nanotube Chemiresistive Sensor Arrays for VOCs. *J. Phys. Chem. C* **2012**, *116*, 3845−3850.

(28) Rushi, A.; Datta, K.; Ghosh, P.; Mulchandani, A.; Shirsat, M. Iron Tetraphenyl Porphyrin Functionalized Single Walled Carbon Nanotubes for Detection of Benzene. *Mater. Lett.* **2013**, *96*, 38−41.

(29) Ndiaye, A.; Bonnet, P.; Pauly, A.; Dubois, M.; Brunet, J.; Varenne, C.; Guerin, K.; Lauron, B. Noncovalent Functionalization of Single-Wall Carbon Nanotubes for the Elaboration of Gas Sensor Dedicated to BTX Type Gases: The Case of Toluene. *J. Phys. Chem. C* **2013**, *117*, 20217−20228.

(30) Macagnano, A.; Sgreccia, E.; Paalesse, R.; Cesare, F.; Amico, A.; Natale, C. Sorption and Condensation Phenomena of Volatile Compounds on Solid-State Metalloporphyrin Films. *Sens. Actuators, B* **2007**, *124*, 260−268.

(31) Arshad, S.; Salleh, M.; Yahaya, M. Quartz Crystal Microbalance Gas Sensor for Detection of Volatile Organic Compounds using Titanium Dioxide coated with Dye-porphyrin. *Solid State Sci. Technol.* **2008**, *16*, 75−84.

(32) Tanaka, H.; Yajima, T.; Matsumoto, T.; Otsuka, Y.; Ogawa, T. Porphyrin Molecular Nanodevices Wired Using Single-Walled Carbon Nanotubes. *Adv. Mater.* **2006**, *18*, 1411−1415.

(33) (a) Wang, Y.; Yeow, J. A Review of Carbon Nanotubes-Based Gas Sensors. *J. Sensors* **2009**, *2009*, 1−24. (b) Zhang, T.; Mubeen, S.; Myung, N.; Deshusses, M. Recent Progress in Carbon Nanotube-Based Gas Sensors. *Nanotechnology* **2008**, *19*, 332001 (14pp).

(34) AlChE: American Institute of Chemical Engineers.http://www3.aiche.org/proceedings/Abstract.aspx?PaperID=69788 (accessed March 13, 2014).
(35) Lim, J.; Phiboolsirichit, N.; Mubeen, S.; Deshusses, M.; Mulchandani, A.; Myung, N. Electrical and Gas Sensing Properties of Polyaniline Functionalized Single-Walled Carbon Nanotubes. *Nanotechnology* **2010**, *21*, 075502 (7pp).
(36) Absorption and Fluorescence Spectroscopy of Tetraphenylporphyrin and Metallo-Tetraphenylporphyrin. http://www.lasalle.edu/~prushan/Abs%20and%20Fluor%20of%20TPPH2.pdf (accessed Aug 1, 2013).
(37) Zhang, T.; Nix, M.; Yoo, B.; Deshusses, M.; Myung, N. Electrochemically Functionalized Single-Walled Carbon Nanotube Gas Sensor. *Electroanalysis* **2006**, *18*, 1153−1158.
(38) Mubeen, S.; Zhang, T.; Chartuprayoon, N.; Rheem, Y.; Mulchandani, A.; Myung, N.; Deshusses, M. Sensitive Detection of H_2S Using Gold Nanoparticles Decorated SWNTs. *Anal. Chem.* **2010**, *82*, 250−257.
(39) Kauffman, D.; Kuzmych, O.; Star, A. Interactions between Single-Walled Carbon Nanotubes and Tetraphenyl Metalloporphyrins: Correlation between Spectroscopic and FET Measurements. *J. Phys. Chem. C* **2007**, *111*, 3539−3543.
(40) Lim, J.; Phiboolsirichit, N.; Mubeen, S.; Deshusses, M.; Mulchandani, A.; Myung, N. Electrical and Sensing Properties of Single-Walled Carbon Nanotubes Network: Effect of Alignment and Selective Breakdown. *Electroanalysis* **2010**, *22*, 99−105.
(41) Mubeen, S.; Lim, J.; Sriangarajan, A.; Mulchandani, A.; Deshusses, M.; Myung, N. Gas Sensing Mechanism of Gold Nanoparticles Decorated Single-Walled Carbon Nanotubes. *Electroanalysis* **2011**, *23*, 2687−2692.
(42) Heller, I.; Janssens, A.; Mannik, J.; Minot, E.; Lemay, S.; Dekker, C. Identifying the Mechanism of Biosensing with Carbon Nanotube Transistors. *Nano Lett.* **2008**, *8*, 591−595.
(43) Bhal, B. S. *Elementary Organic Chemistry: A Modern Approach*; S. Chand Publication: New Delhi, India, 1987.